Photoelectrochemical Etching of InAs

Derek Harris,*[a] Paul A. Kohl,* and Jack Winnick*

School of Chemical Engineering, Georgia Institute of Technology, Atlanta, Georgia 30332-0100

ABSTRACT

Photoelectrochemical etching of n-InAs (E_g = 0.36 eV) is demonstrated. Although the concentration of thermally generated minority carriers and saturation current are high compared to larger bandgap semiconductors, photocurrent to dark current ratios as high as 4:1 were obtained at low temperature (2°C) and at potentials near the flatband potential. A surface film primarily composed of arsenic oxide was formed during oxidative decomposition of the semiconductor and plays a role in the rate of dissolution and in the current-voltage response. In 0.2*M* H_2SO_4, 6 electrons per InAs were involved in the oxidation dissolution, while only 4 electrons per InAs were found in 0.2*M* HCl because of the formation of In(I)-chloride species.

Interest in the processing of III-V semiconductors has grown as the variety of devices using the materials has increased. III-V semiconductors are particularly well suited for use in optoelectronic devices such as light-emitting diodes (LEDs), photodetectors, and lasers because of their direct bandgap. InAs has been used for tunnel diode heterostructures in microwave applications such as high speed digital switches and frequency locking circuits.[1-5] InAs has a high carrier mobility and large offset of the conduction and valence bands from other III-V materials that makes it ideal for use in quantum-well structures. These types of devices present many opportunities for photoelectrochemical (PEC) etching of InAs.[6]

PEC processing is the selective reaction of an illuminated semiconductor in contact with an electrolyte. N-type semiconductors can be oxidized selectively by photo-induced hole-initiated oxidation of the lattice leading to the dissolution of the semiconductor in the illuminated regions. The surface of a p-type semiconductor can be reduced selectively by using photogenerated electrons in the conduction band.

PEC etching has several advantages over more conventional processing techniques;[6] (*i*) PEC processing uses low energy reactants (photons whose energy is greater than the semiconductor bandgap) as opposed to the high energy plasmas used in dry etching, so that damage-free processing can be achieved; (*ii*) the rate of reaction is directly proportional to the illumination intensity so that spatial variations in the light intensity lead to the same spatial variations in the etch rate; (*iii*) different materials can be etched selectively by using a light source with a wavelength specific to the particular bandgap. This is particularly useful for processing multilayered heterostructures; (*iv*) the processing can be made specific to the dopant type (n or p) because photogenerated minority carriers are one of the reactants; (*v*) the electrical current is directly proportional to the etch rate so that the progress of the etch can be monitored easily. The reaction for InAs can be expressed as

$$InAs + (6 - x)h^+ \rightarrow In^{3+} + As^{3+} + xe^- \quad [1]$$

In photoetching n-type semiconductors, photogenerated holes migrate to the semiconductor-solution interface where they represent a missing electron in the bonding orbital of the crystal, thus weakening the bond of the semiconductor. This leads to the dissolution of the semiconductor crystal.

Photoelectrochemical etching has been used to produce structures in n-GaAs [7-10] and n-InP [11-13] devices. Integral lenses have been fabricated on InP LEDs,[14] and PEC etching has been used to make diffraction gratings in n-InP with periods as fine as 235 nm for distributed feedback lasers.[15] PEC etching also has been demonstrated for p-GaAs and p-InP. The illumination of a p-type semiconductor biased negative of the flatband potential, leads to a high concentration of electrons at the semiconductor surface. A two-step etching procedure was investigated because the reduction of the III-V semiconductors does not lead to the formation of soluble products.[14]

The PEC etch rate and spatial resolution can be limited by the dissolution rate of the reaction products, or by the thermal generation of charge carriers. Either may cause dissolution of the semiconductor in nonilluminated areas. Thermally generated carriers are especially important with the smaller bandgap semiconductors, such as InAs. Previously, the small photocurrents observed for InAs were attributed to its small bandgap.[16]

The feasibility of PEC etching InAs is investigated here, focusing particularly on the dissolution of the products and the effect of thermally generated carriers.

Experimental

The electrochemical experiments were carried out using a conventional three-electrode cell with an optically flat window for illumination of the semiconductor electrode. The counterelectrode was a platinum wire; a saturated calomel electrode (SCE) was used as the reference. High purity nitrogen was used to deaerate the solutions and spectroscopic grade water from Aldrich was used for preparing the solutions. All other chemicals were reagent grade. A Princeton Applied Research (PAR) Model 273 electrochemical system was used to perform cyclic voltammetry and chronoamperometry. The (100) n- and p-InAs crystals were obtained from MCP Electronics Materials Ltd., Berkshire, England. An electrical contact was made on the back side of the InAs crystal with an indium-gallium alloy and silver paint. The copper rod and edges of the crystal were insulated from the solution with Apiezon W wax and nonconductive epoxy.

The electrodes were illuminated with a 10 mW He-Ne laser. The topographical profile of the etched holes was measured with a Tencor Alpha Step surface profilometer. Auger electron spectroscopy (AES) measurements of the

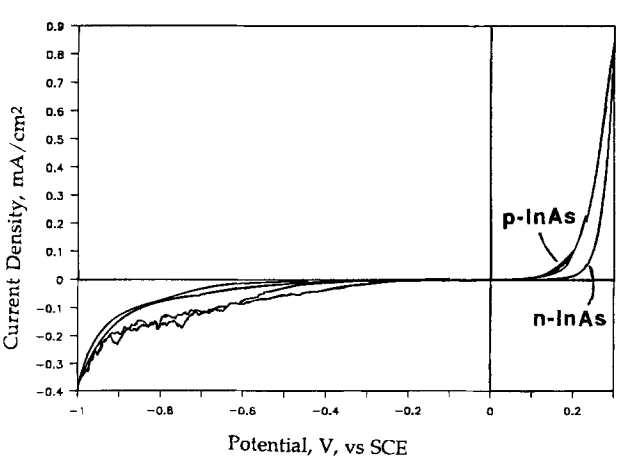

Fig. 1. Cyclic voltammogram for n- and p-InAs in 0.2*M* H_2SO_4.

* Electrochemical Society Active Member.

[a] Present address: IBM Corporation, Hopewell Junction, NY 12533-6531.

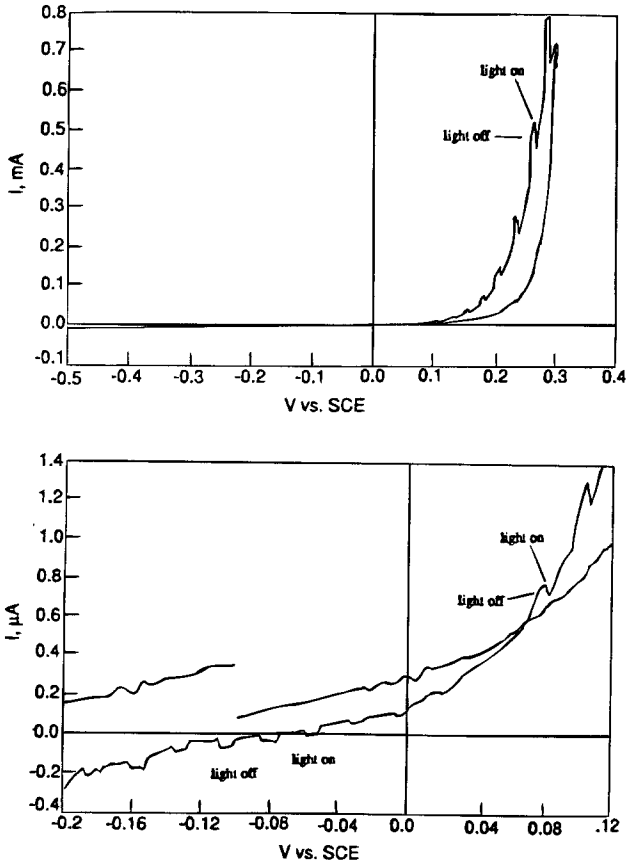

Fig. 2. (a, top) Photo-oxidation of n-InAs in 0.2*M* H_2SO_4; (b, bottom) detail of photoreduction and oxidation.

InAs surfaces oxidized under different conditions were made with a Physical Electronics 601 Auger electron spectrometer. A control sample also was analyzed to determine the relative strength of the In and As signals so that a depth profile of the In to As ratio was obtained.

Results

The I-V behavior of n- and p-InAs in 0.2*M* H_2SO_4 in the dark are shown in Fig. 1. The oxidation current increased at potentials positive of 0.10 V *vs.* SCE for both dopant types. At these potentials, the current is proportional to the concentration of valence band holes at the semiconductor-solution interface. The reduction current negative of −0.7 V was similar for both n- and p-InAs in the dark. There was also no difference in the I-V for n-InAs in 0.2*M* HCl and 0.2*M* H_2SO_4. The oxidation current was dependent on the previous oxidation and reduction history of the InAs. The magnitude of the oxidation current decreased on succeeding scans when the positive extreme of the potential scans was 0.2 to 0.3 V. Auger surface analysis showed that the slow dissolution and precipitation of the arsenic oxidation products is responsible for the decrease in the current. The large oxidation current then may be restored by reducing the surface. When the switching potential for the positive-going scan was 0.3 V, and −1.0 V on the negative-going scan, the oxidation current was greater on the subsequent scans.

The number of electrons observed in the external circuit, given as 6 in Eq. 6, was calculated by integrating the current (in the absence of illumination), and measuring the volume of material etched. In H_2SO_4, 6.2 electrons were observed and in HCl, 4.3 electrons per InAs were measured. This lower number for HCl is similar to the results of Hsieh and Shih[17] who detected In(I)-chloro complexes in the dissolution products.

The oxidative photocurrent for n-InAs is shown in Fig. 2, where the semiconductor was illuminated with a chopped white light source. The flatband potential, V_{FB}, of n-InAs was taken as the most negative potential where the photo-oxidation was observed, approximately 0.10 V *vs.* SCE in 0.2*M* H_2SO_4 at 25°C. The photo-oxidation starts at approximately the same potential as the dark oxidation, as shown in Fig. 2a. There was no potential region in which the photocurrent was observed without a dark current background. The dark current arises from thermally generated holes.

In addition to the photo-oxidation current, a small photocathodic current was observed on the negative-going scan, following the oxidation process, Fig. 2b. This unusual photocurrent is most likely related to undissolved oxidation products produced on the positive-going scan.

I-V measurements were made in H_2SO_4 at three different temperatures 2, 26, and 52°C. The photo-oxidation did not change with temperature; however, the photoreduction was a function of temperature. The magnitude of the photoreduction measured at 0.1 V *vs.* SCE was 5 μA/cm^2 at 2°C, 12.5 μA/cm^2 at 26°C, and 37.5 μA/cm^2 at 52°C. The potential at which the photo-oxidation changed to a photoreduction on the negative-going scan, following a positive scan was dependent on the temperature. At 2°C the switch was at *ca.* 0.04 V *vs.* SCE and at 52°C it was at 0.10 V *vs.* SCE.

The photoreduction current for p-InAs started at *ca.* 0.16 V, similar to that for n-InAs; however, the magnitude of the current was much larger, as shown in Fig. 3. The photocurrent was much greater on the negative-going scan following a positive-going scan where the semiconductor surface was oxidized. The photocathodic current is most likely due to the reduction of hydrogen ions because no degradation of the semiconductor was observed.

To determine whether a useful photo-to-dark etch rate may be achieved, several experiments were conducted. The InAs electrodes were immersed in either HCl or H_2SO_4, biased at different anodic potentials and etched for 20 min while the current was monitored. The comparison to p-InAs was made because of its high hole concentration in the absence of illumination. An HeNe laser was used for n-InAs so that the dark and illuminated etch rates are measured in one experiment. By periodically blocking the illumination, the photocurrent and dark current may be recorded. The data for n-InAs in 0.2*M* H_2SO_4 is shown in Table I.

The etch rate in the dark for n- and p-InAs biased at 0.3 V in 0.2*M* H_2SO_4 was approximately the same, 0.175 μm/min at 2°C, 0.625 μm/min at 26°C, and 1.7 μm/min at 52°C. The etched surfaces were relatively smooth. In 0.2*M* HCl, the dark etch rate increased to 0.7 μm/min for p-InAs and 1.1 μm/min for n-InAs, however, the InAs surface was significantly rougher than that etched in H_2SO_4.

A larger difference in the n-InAs photoetch rate in H_2SO_4 and HCl was observed. The photoetch rates in 0.2*M* H_2SO_4 using the HeNe laser were 0.45, 0.5, and 0.3 μm/min at 2, 26, and 52°C, respectively. The sample surfaces were still specularly reflective after etching demonstrating the smooth topography. The laser etched hole had a Gaussian

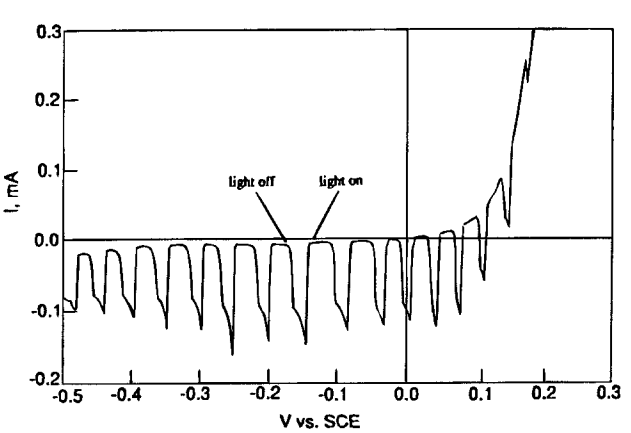

Fig. 3. Photoreduction of p-InAs in 0.2*M* H_2SO_4.

Table I. n-InAs etch rates (μm/min).

	Bias potential								
	0.15			0.225			0.3		
T (°C)	Dark	Light	L/D	Dark	Light	L/D	Dark	Light	L/D
2	0.0075	0.03	4/1	0.03	0.065	2.2/1	0.175	0.4	2.7/1
26	0.05	0.035	0.7/1	0.25	0.3	1.2/1	0.625	0.5	0.8/1
50	0.125	0	0	0.5	0.1	0.2/1	1.7	0.3	0.18/1

profile, similar to the profile of the laser. The light-to-dark etch rate ratio (L/D), a measure of the selectivity, using the HeNe laser is shown in Table I. The largest ratio, 4:1, was obtained at 2°C. The hole etched in 0.2*M* HCl at 0.3 V was shallow with a photoenhanced etch rate of only 0.085 μm/min at room temperature, far less than the dark etch rate.

The L/D ratio was a strong function of potential and temperature. No photoetching was observed when n-InAs was biased at 0.15 V and 52°C. The dark etch rate increased with an increase in potential, as expected from Fig. 1, or temperature. The photoetch rate, however, had a much greater dependence on potential than temperature.

The current densities for the etching experiments listed in Table I, are shown in Table II. They clearly show the dependency of photocurrent on temperature and potential. At 52°C the photocurrent was small in comparison to the dark current and within the noise of the dark current. This shows that the concentration of photogenerated holes was insignificant in comparison to that of thermally generated holes at the higher temperatures, while at lower temperatures, a more desirable photocurrent-to-dark current ratio is obtained.

To investigate the surface effects observed after oxidation of InAs, AES analysis was performed on the n-InAs oxidized at 0.3 V in 0.2*M* HCl and 0.2*M* H_2SO_4 at 26°C. An arsenic and oxygen-rich surface layer was found on both InAs samples, indicating the presence of an arsenic oxide layer, as shown in Fig. 4. After a brief sputtering etch for 15 s, the In-to-As ratio for the crystal etched in HCl had returned too close to that of the reference crystal. The sputter-etching was calibrated to etch thermally grown SiO_2 at a rate of 60 Å/min. After 30 s there was virtually no difference between the reference InAs and the InAs etched in HCl. The crystal etched in H_2SO_4 was sputtered for 5 min and was not through the arsenic-rich surface film.

Discussion

To optimize the etch rate and photoetching selectivity, we must understand in more detail the mechanism and rate-limiting steps with the dark and photocurrent. The hole oxidation current, Eq. 1, is proportional to the number of holes at the semiconductor-solution interface. For n-type semiconductors, the hole concentration at the semiconductor surface, N_S, is exponentially dependent on the potential for potentials positive of V_{FB}, as given by Eq. 2

$$N_S = N_a \exp [q(V - V_{FB})/kT] \quad [2]$$

where N_a is the hole concentration in the semiconductor bulk, N_S is the hole concentration at the semiconductor solution interface, q is the magnitude of the electronic charge, V is the electrode potential, k is the Boltzmann constant, and T is the temperature.

At potentials positive of V_{FB} for n-InAs, or negative of V_{FB} for p-InAs, the maximum dark current, I_{sat}, is controlled by the thermal generation and diffusion of minority carriers over the diffusion length of the carrier, as given in Eq. 3 for n-type carriers[18]

$$i_{sat} = q \frac{n_i^2}{N_D} \sqrt{\frac{kT}{m_p}} \quad [3]$$

where m_p is the effective mass of holes, n_i is the intrinsic carrier concentration, and n_D is the dopant density. i_{sat} for the n-InAs used in this study was 45.8 A/cm^2, and the highest currents measured were below 0.02 A/cm^2. i_{sat} for p-InAs was 16.7 A/cm^2 which is far greater than the currents measured here. In larger bandgap semiconductors, i_{sat} is very small (*e.g.*, <1 μA/cm^2) so that thermally generated minority carriers do not play a significant role.

There are several aspects of the dissolution reaction which are temperature dependent: the thermal generation of holes, the activity of the dissolution products, and the solubility of the solution species in the electrolyte. The ratio of hole concentration at 325 K to the hole concentration at 275 K, calculated from Eq. 2, is used as a measure of the effect of temperature on the hole concentration and is shown in Fig. 5 *vs.* the potential drop across the space charge region. The ratio starts at close to 20 near the flat-band potential and decreases as the bands bend. At higher band bending, the concentration of thermally generated carriers at the semiconductor-solution interface increases so that the ratio of photogenerated carriers to thermally generated carriers is smaller (for fixed illumination).

The ratio of the observed steady-state dark currents at 325 K to those at 275 K for n-InAs etched in 0.2*M* H_2SO_4 are plotted in Fig. 5. The ratios were calculated taking into account the small difference in V_{FB} at different temperatures. Thus, the current density ratios clearly follow the surface hole concentration, as expected because the reaction is directly dependent on the surface hole concentration, Eq. 1.

During the steady-state oxidation experiments, the AES measurements show that an arsenic oxide-rich surface film is formed. The rate of solvation of the indium products is greater than that of the arsenic products leaving an arsenic oxide film. The semiconductor-oxide interface appears to cause the unexpected photoeffects on the negative-going potential scans following the oxidation of the surface.

The rate of dissolution of arsenic oxide increases with temperature because of an increase in the solubility of arsenic oxide,[20] as well as an increase in the diffusion coefficient and decrease in the viscosity of water.[19]

Table II. Oxidation currents for n-InAs.

	Bias potential					
	0.15		0.225		0.3	
T (°C)	Dark	Light	Dark	Light	Dark	Light
2	0.009	0.46	0.64	4.4	4	9.4
26	0.25	0.51	5.4	3.8	14.3	10.2
50	2.3		10		37.5	

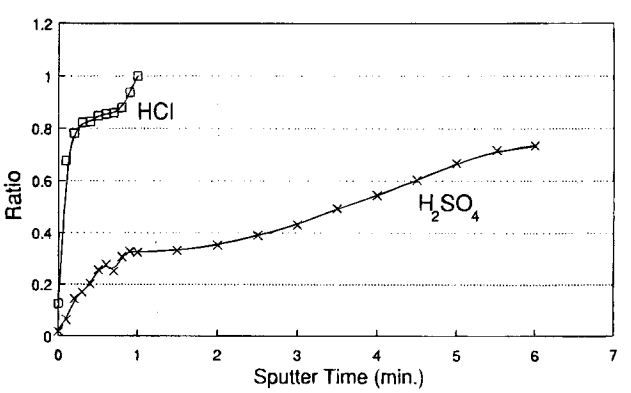

Fig. 4. Ratio of In to As by AES *vs.* sputter time for n-InAs oxidized in 0.2*M* HCl and 0.2*M* H_2SO_4.

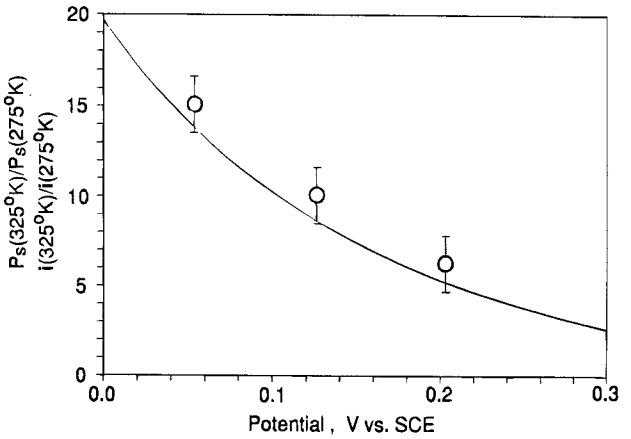

Fig. 5. Ratio of calculated surface hole concentrations 325/275 K (—), ratio of steady-state etch currents 325/275 K (○).

Here, the temperature was increased from 275 to 325 K; for these temperatures the viscosity of water decreases from 1.636 to 0.542 cP. When coupled with an increase in the diffusivity by more than a factor of three, one expects a doubling of the diffusion limited current prior to the onset of precipitation. The solubility of the arsenic oxide also increases with temperature, as shown in Table III.[20] For the temperature extremes used here, the solubility of the As_2O_3 increases by a factor of three. Thus, the observed current density for the oxidation-dissolution reaction of InAs is greater at higher temperatures because of the higher generation of reactants (holes) as well as the removal of products.

The steady-state photo-oxidation current is not affected by temperature to the same extent as the dark current. Tables I and II show that the photoetching rate and photocurrent increased only slightly when the temperature was increased from 275 to 298 K and actually decreased at the highest temperature because the generation of electron-hole pairs by photons is not dependent on temperature. The profiles of the holes etched at the higher temperatures were much wider than those at lower temperatures and not as clearly defined. This may indicate that at the higher temperatures the oxidation rate of the various crystal faces may be different.

The etching experiments showed that the dark etch rate increased dramatically when HCl was the electrolyte as opposed to H_2SO_4. The indium was solvated without being oxidized to In(III) through the formation of stable complexes with Cl^- ions in solution. The stability of indium-chloride species has been investigated previously.[21] The formation of In(I) leads to only 4 electrons transferred per molecule of InAs dissolved. The presence of chloride also improves the dissolution of arsenic oxide, as seen in the Auger results.

Summary

The etching of InAs is controlled by the concentration of holes at the semiconductor-solution interface and dissolution of the oxidation products. The dark current and oxidation rate of InAs increased with temperature and the use of HCl as the electrolyte. Selective photoetching has been shown for n-InAs through the photoanodic oxidation of the semiconductor lattice even though the concentration of thermally generated charge carriers is large. The largest photoetching selectivities were found in $0.2M$ H_2SO_4 and at the lowest bias potentials and lowest temperatures (0.15 V *vs.* SCE and 2°C). Lowering the temperature and potential decreased the concentration of thermally generated charge carriers at the semiconductor-solution interface. The highest photoetching selectivities (light to dark etching) was 4 to 1.

The dark etch rate was affected by the formation of an As-rich oxide film on the surface of the InAs. Raising the temperature speeds the dissolution of this film. The addition of Cl^- also increased the dissolution of this film and decreased the number of charge carriers for the reaction from 6 to H_2SO_4 to 4 for HCl because of the formation of an In(I)-chloride complex.

Table III. Solubility of As_2O_3 in Water.[20]

	As_2O_3 (g/100 g water)							
Temperature (°C)	0	10	20	30	40	60	80	100
As_2O_3 (g)	1.20	1.49	1.82	2.31	2.93	4.31	6.11	8.2

Manuscript submitted Aug. 5, 1993; revised manuscript received Jan. 12, 1994.

Georgia Institute of Technology assisted in meeting the publication costs of this article.

REFERENCES

1. D. H. Chow, J. R. Soderstrom, D. A. Collins, D. Z.-Y. Ting, E. T. Yu, and T. C. McGill, *Quantum-Well and Superlattice Physics III,* Vol. 1283, p. 2, SPIE, Bellingham, WA (1990).
2. L. F. Luo, R. Beresford, and W. I. Wang, *Appl. Phys. Lett.*, **53,** 2320 (1988).
3. L. F. Luo, R. Beresford, and W. I. Wang, *ibid.*, **55,** 2023 (1989).
4. J. Werking, G. Tuttle, C. Nguyen, E. L. Hu, and H. Kroemer, *ibid.*, **57,** 905 (1990).
5. E. R. Brown, J. R. Soderstrom, C. D. Parker, L. J. Mahoney, K. M. Molvar, and T. C. McGill, *ibid.*, **58,** 2291 (1991).
6. P. A. Kohl and D. B. Harris, *Electrochim. Acta,* **38,** 101 (1993).
7. S. Mottet and L. Henry, *Electron. Lett.*, **19,** 920 (1983).
8. D. V. Podlesnik, H. H. Gilgen, R. M. Osgood, and A. Sanchez, *Appl. Phys. Lett.*, **43,** 1083 (1983).
9. M. M. Carrabba, N. M. Nguyen, and R. D. Rauh, *This Journal,* **134,** 1855 (1987).
10. V. Svorcik, V. Rybka, and V. Myslik, *Chem. Phys. Lett.*, **144,** 548 (1988).
11. J. E. Bowers, B. R. Hemenway, and D. P. Wilt, *Appl. Phys. Lett.*, **46,** 453 (1985).
12. D. Moutonnet, *Mater. Lett.*, **6,** 443 (1988).
13. R. M. Lum, F. W. Ostermayer, Jr., P. A. Kohl, A. M. Glass, and A. A. Ballman, *Appl. Phys. Lett.*, **47,** 269 (1985).
14. P. A. Kohl and F. W. Ostermayer Jr., *Annu. Rev. Mater. Sci.*, **19,** 389 (1989).
15. F. W. Ostermayer, Jr. and P. A. Kohl, *Appl. Phys. Lett.*, **39,** 76 (1981).
16. S. Menezes, B. Miller, and K. J. Bachman, *J. Vac. Sci. Technol.*, **B1,** 51 (1983).
17. H. F. Hsieh and H. S. Shih, *This Journal,* **137,** 1348 (1990).
18. H. Gerischer, in *Physical Chemistry: An Advanced Treatise,* Vol. IXA, H. Eyring, Editor, Academic Press, New York (1970).
19. R. C. Reid, J. M. Prausnitz, and B. E. Poling, *The Properties of Gases and Liquids,* 4th ed., pp. 388-440, McGraw-Hill, New York (1987).
20. *Lange's Handbook of Chemistry,* 12 ed., J. A. Dean, Editor, McGraw-Hill, New York (1979).
21. A. M. Bond, *This Journal,* **119,** 1503 (1972).